Authors version
DOI: 10.1021/acs.jpcc.8b01070
J. Phys. Chem. C

Analysis of the Influence of Selective Contact Heterojunctions on the Performance of Perovskite Solar Cells

Manuel García-Rosell,[1] Agustín Bou,[2] Juan A. Jiménez-Tejada,[1] Juan Bisquert*[2], Pilar Lopez-Varo*,[1]

Departamento de Electrónica y Tecnología de Computadores, CITIC-UGR, Universidad de Granada, 18071 Granada, Spain

Institute of Advanced Materials (INAM), Universitat Jaume I, 12006 Castelló, Spain

E-mail: bisquert@uji.es, pilarlopez@ugr.es

Abstract

Knowledge of the mechanisms that take place at the selective contacts, located at the charge-transport-layer (CTL)/perovskite heterojunctions, is crucial for the optimization of perovskite solar cells. Anomalous high values of the low-frequency capacitance at open-circuit and short-circuit indicate a high accumulation of charge at the interfaces, which could hinder the extraction of charge and increase hysteresis in current-voltage curve. To investigate this issue, we develop a simulation model based on the drift-diffusion differential equations with specific boundary conditions at the interfaces. We have simulated the CTL/perovskite structures as part of the entire perovskite solar cell, in order to establish the realistic energy profile across the interface. The energy profile allows to detect in which situations free charge accumulation at the interfaces exists, and to quantify this accumulation as a function of the device and material parameters. We discuss the role and the importance of each CTL/perovskite interface at open-circuit and short-circuit. We conclude that the accumulation of charge at the interfaces is strongly affected by the specific contact materials, and critically depends on a compromise between the presence of ions, the values of the carrier mobility, and the interfacial and bulk recombination parameters.

1. Introduction

Perovskite solar cells (PSCs) have disrupted the scene of the present photovoltaic research with their highly impressive power conversion efficiencies.[1-4] Notwithstanding the significant advances in the PSC performance, a range of new experiments made on PSCs try to find out what physical mechanisms govern their photovoltaic conversion, including characteristic phenomena such as hysteresis in current-voltage curves[5] or extremely high values of the low-frequency capacitance.[6,7] As the transport mechanisms do not seem to be the bottleneck in the flow of the current, other constituents of the device structure, such as heterojunctions and interfaces, can affect the whole PSC performance.[2,8] In fact, interfacial engineering is essential to improve the efficiency through better charge collection and a reduction in charge recombination.[9] Different experiments provide clear evidence about the importance of the interfaces between the charge transport layers (CTLs) and the perovskite semiconductor. Nanometer-scale-profiling measurements show how the main electric potential drops in the TCO-TiO_2/perovskite contact region, either in the planar or in the mesoporous perovskite solar cells.[10-12] Anomalous experimental transient results are also attributed to the role of these interfaces.[13,14]

Accumulation of free charge at the CTL/perovskite interfaces has been suggested as a dominant mechanism causing the hysteresis observed in current-voltage curves.[5,15] This accumulation can affect the extraction of charge at the interfaces, and thereby the efficiency of the PSC.[8] In conjunction with experimental observations, numerical modeling has been useful to elucidate the PSC behavior.[2]

Different numerical simulation models have interpreted successfully hysteresis observed in experimental current-voltage curves,[5,15-19] and some of these models include ion migration.[5,15] There is a broad consensus in the scientific community that ion motion is one of the major factors that affect the performance of PSCs.[8,14,20] Senocrate et al.[21] have recently applied a full battery of solid state electrochemistry methods to identify the dominant ionic species in lead halide perovskites. Li et al.[22] observed the suppression of luminescence by ionic displacement, correlated with direct identification of ionic distribution. Theoretical works have determined two main effects of the ionic migration on the performance of PSCs.[8] One effect comes from the accumulation of ions at the interfaces by applied bias or illumination, which leads to experimentally observed slow charging, capacitive responses and hysteresis in current-voltage curves.[23] Another consequence is the modification, or even screening, of the electric field distribution in the perovskite semiconductor entailing a variation in the charge collection.[8]

A physical effect often considered in models is electronic charge traps at the interfaces, serving as recombination centers.[5,15,24] For the recombination process to be noticeable, a high accumulation of free charge is necessary at the interfaces. Models applied to p-type/intrinsic/n-type (p-i-n) heterojunction solar cells manage to reproduce

a high accumulation of free charge only after the PSC has undergone a bias treatment.[5,15] This treatment induces an ionic charge distribution along the perovskite that attracts free charges toward the interfaces. In these simulations, the accumulation of charge does not appear under steady state conditions without bias pretreatment, i.e. in steady open-circuit (OC) or short-circuit (SC) conditions. However, a high accumulation of charge has been detected in these operating conditions by capacitance measurements showing huge values of the capacitance at low frequency[6,7] strongly dependent of the contact material.[6,25] In this regard, more work is needed in order to explain these anomalous values of the capacitance at open and short-circuit conditions.

Accumulation of charge has been observed in previous numerical simulation in PSCs operating at OC.[26] However, the detailed electronic distribution structure of electron transport layer (ETL) or (HTL) has not been considered in previous works. It has been widely recognized that the photophysical response of PSC is strongly affected by the specific contact materials. For example, in the typical $TiO_2/CH_3NH_3PbI_3$/spiro-OMeTAD version of the PSC, electronic distribution in TiO_2 and spiro-OMeTAD layers can provide an array of significant physical effects.[9,10,27,28] Therefore, in this paper we extend previous drift-diffusion models with a full description of band bending and charge distribution in the contact layers, as presented initially in Figure 1. Here we focus on the planar configuration and the effect of mesoporous layer is discussed by Gagliardi et al.[29]

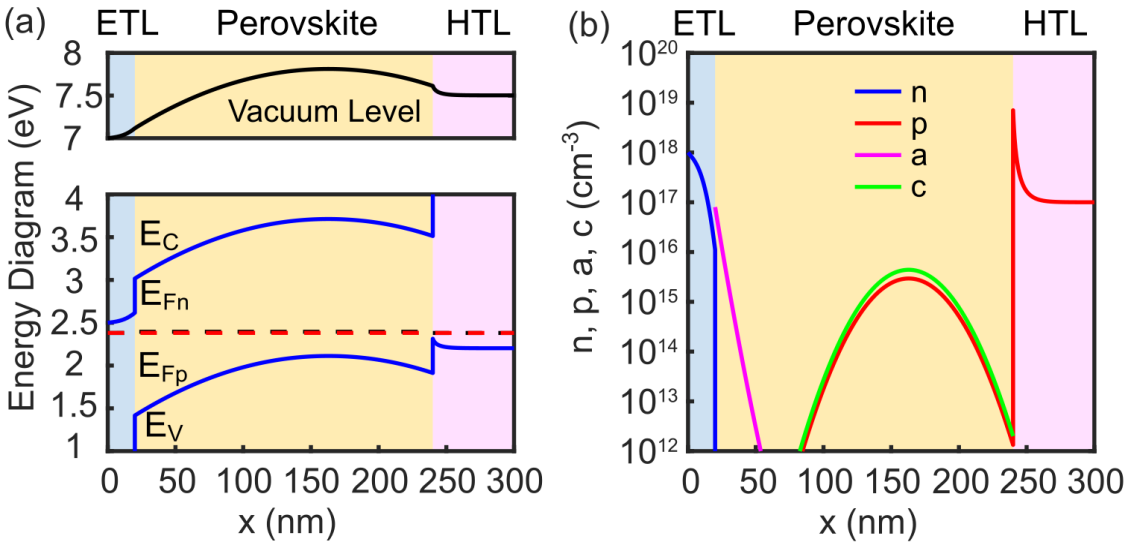

Figure 1. (a) Energy diagram of the ETL/p-type-perovskite/HTL structure working in darkness and equilibrium ($V_{app} = 0\,\mathrm{V}$). (b) Distributions of electrons (n), holes (p), anions (a^-) and cations (c^+) along the structure. The n-type ETL, p-type perovskite and p-type HTL are simulated with donor density $N_{D,ETL} = 10^{18}\,\mathrm{cm}^{-3}$, and acceptor densities $N_A = 10^{17}\,\mathrm{cm}^{-3}$ and $N_{A,HTL} = 10^{17}\,\mathrm{cm}^{-3}$, respectively. A low on-average concentration of mobile ions of $N_{ion} = 10^{15}\,\mathrm{cm}^{-3}$ is considered in the perovskite.

In Section 2, we describe the methods to model the CTL/perovskite heterostructures. In Sections 3 and 4, we analyze these two interfaces at OC and SC conditions, respectively, in order to detect whether free charges accumulate at the interfaces of these heterostructures, as pointed out in capacitance measurements.[6] In this analysis, different parameters are taken into account: the presence or not of ions in the perovskite, the value of the energy steps of the minimum of the conduction band and maximum of the valence bands at the CTL/perovskite interfaces, the carrier mobility in the perovskite, the relative permittivity of the CTLs, and the interfacial and bulk recombination.

2. Theory

In our numerical model, the transport equations are considered, as already described by Lopez-Varo et al. in previous works,[2,8,26] but now adapted to the ETL/perovskite/HTL structure shown in Figure 1. The parameters used in the simulation are representative values.[2] We take as a reference the ordinary planar three-layered configuration $TiO_2/CH_3NH_3PbI_3$/spiro-OMeTAD. Following recent detailed investigations,[2,21] we assume that $CH_3NH_3PbI_3$ is predominantly p-doped by iodine interstitials. However, n-type or intrinsic-type perovskites can also be found depending on the preparation method or on the presence of impurities. The energy diagram of a heterostructure formed by an n-type ETL, a p-type perovskite and a p-type HTL in darkness and equilibrium is shown in Figure 1a. The analysis of an n-type perovskite can be seen in SI (Section 4). The results are quite similar to those shown here for the p-type perovskite, only that the role of the contacts is inverted, as one would expect from basic semiconductor concepts.

The main ionic conductivity in $CH_3NH_3PbI_3$ is associated to iodine vacancies.[21] Nevertheless, we consider that both anions and cations can migrate inside the perovskite layer. The method considers variable densities of electrons (*n*) and holes (*p*) in any of the three layers, and the density of anions (a^-) and cations (c^+) in the perovskite semiconductor, and their respective currents J_n, J_p, J_a and J_c. Therefore, any desired configuration of doping and energy levels can be investigated by a similar approach.

The numerical model considers:[2] (1) *Drift-diffusion mechanisms* for the motion of free charge carriers through the whole structure, (2) *Drift-diffusion mechanisms* for the motion of ions only in the perovskite semiconductor, (3) *Poisson's equation* for the electric potential, (4) the *perovskite* material as a *p-type semiconductor*, (5) *Fermi statistic*, which includes the possible degeneration of the perovskite semiconductor when a high accumulation of charge occurs,[26] (6) *bulk recombination* in the perovskite, and (7) *interfacial recombination* between electrons and holes accumulated at the interfaces under test. The interfacial recombination takes place between electrons and holes located in thin layers of ~1-5 nm at each side of the CTL/perovskite interface.[16]

The set of transport equations for electrons, holes and ions have been numerically solved throughout the whole structure using, on the one hand, the typical boundary conditions at metal-semiconductor interfaces[30] (see supporting information, SI) and, on the other hand, the boundary conditions at the CTL/perovskite interfaces, which impose

the continuity of the potential, the current density and the electric displacement at the ETL/perovskite and perovskite/HTL heterojunctions. The continuity of electric displacement, D_i, implies the following relations between the permittivity, ε_i, and the electric field, F_i:

$$D_1 = D_2, \quad \varepsilon_{r1} F_1 = \varepsilon_{r2} F_2 . \tag{1}$$

$$D_2 = D_3, \quad \varepsilon_{r2} F_2 = \varepsilon_{r3} F_3 . \tag{2}$$

where the subindex, $i = 1,2,3$, indicates the layer: ETL → 1, perovskite → 2 and HTL → 3.

Finally, continuity in the pseudo-Fermi levels at the interfaces is also imposed. This condition, combined with the differences in the electron affinity and ionization potential between the materials, implies a discontinuity in the free charge density at these interfaces. The discontinuities in the hole density and in the electron density are given in terms of the steps in the ionization potential ΔE_V and electron affinity ΔE_C at the interface of the layers i and $i+1$ ($i = 1, 2$):

$$\begin{aligned} p_i &= p_{i+1} \exp\left(-\Delta E_V / k_B T\right) \\ n_i &= n_{i+1} \exp\left(-\Delta E_C / k_B T\right). \end{aligned} \tag{3}$$

3. Results and Discussions

3.1. Open-circuit Condition

As stated in the Introduction, the objectives of this work are to establish the potential profile at the CTL/perovskite interfaces, as the energy barriers may determine charge extraction, and to detect the existence of free charge accumulation at these CTL/perovskite interfaces as a function of the device and material parameters. The working conditions to be tested are OC and SC, under illumination and assuming homogeneous light absorption, as capacitance measurements taken just in these conditions have detected high values of the capacitance at low frequencies.[6]

Figure 2a shows the energy diagram of the ETL/perovskite/HTL structure at OC in presence of mobile anions and cations with an on-average concentration $N_{ion} \equiv N_{cation} = N_{anion} = 5 \times 10^{17}\ \mathrm{cm}^{-3}$. The distributions of anion and cation densities in steady state are represented in Figure 2b. The values of the parameters used in the simulation can be found in SI (Table S1). The energy diagram in Figure 2a indicates a high accumulation of free charges at both CTL/perovskite interfaces. The magnitude of the free charge density is represented in Figure 2b. At the ETL/perovskite interface, electrons accumulate in the ETL and holes in the perovskite. At the perovskite/HTL interface, electrons accumulate in the perovskite and holes in the HTL.

The accumulation of the electronic charge can be attributed to different properties of contact selectivity.[31] The quantity of the accumulated charge at the interfaces can be used in order to analyze the effect of different device parameters. The effect of mobile ions is considered in the first place. The relative value between mobile ion concentration

and fixed dopant concentration is an important factor in the operation of the perovskite solar cell. This feature has been studied by extensive numerical simulation by Lopez-Varo et al.[2] Figure 3 compares the distribution of the free carrier densities when mobile ions are absent from the perovskite (dashed lines) or present in concentration $N_{ion} = 5\times10^{17}$ cm^{-3}, like in Figure 2 (solid lines). This comparison shows how the presence of mobile ions causes a decrease of the accumulation of holes in the perovskite at the ETL/perovskite interface and electrons in the perovskite at the perovskite/HTL interface. On the contrary, the accumulation of electrons in the ETL and holes in the HTL increases. This is consistent with the role that mobile ions play in the slow dynamic processes and the accumulation of charge detected in open-circuit voltage decay (OCVD) experiments.[17] The distributions of mobile cations and anions (Figure 2b) are almost uniform throughout the whole bulk of the perovskite, giving rise to a low net ionic charge, and thus, to a low induced electric field.[8]

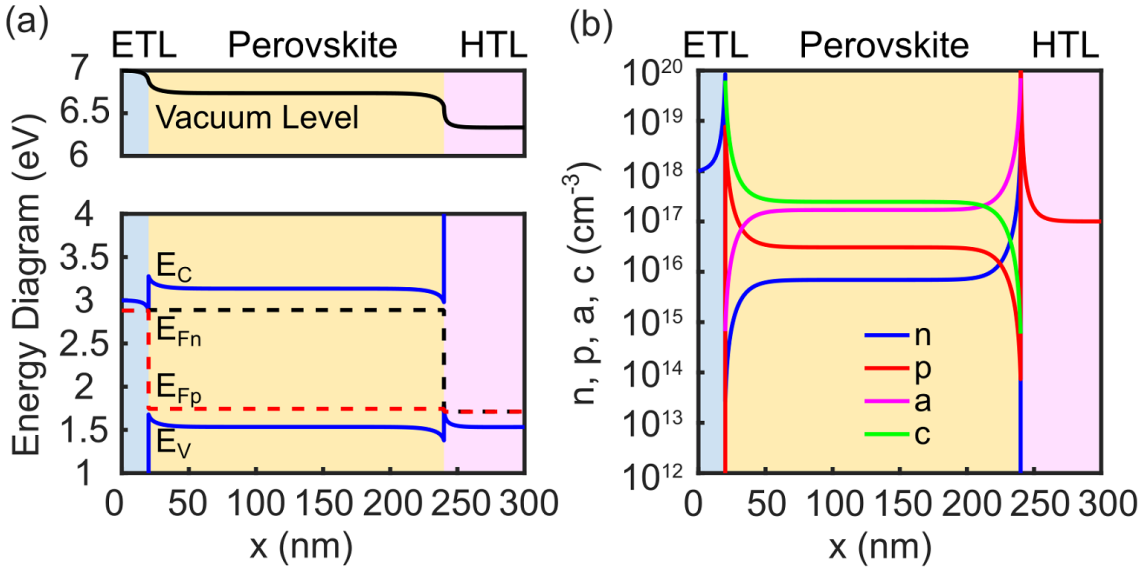

Figure 2. (a) Energy diagram of an ETL/perovskite/HTL structure at OC steady-state. (b) Distributions of electrons, holes and mobile ions along the structure. A high on-average concentration of mobile ions of $N_{ion} = 5\times10^{17}$ cm^{-3} is considered in the perovskite.

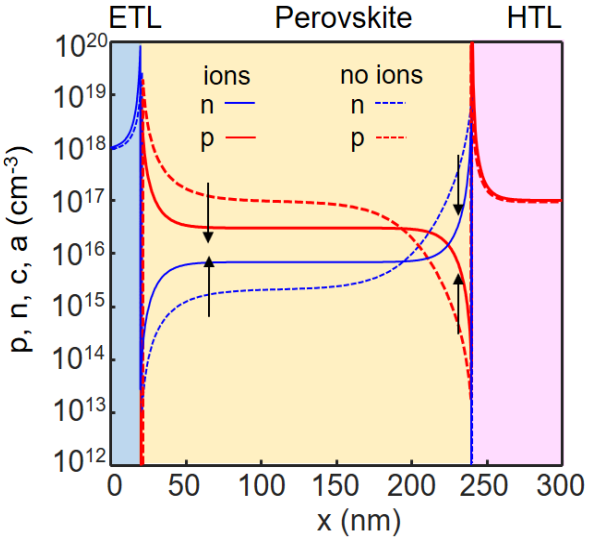

Figure 3. Distribution of free charge carriers along the ETL/perovskite/HTL structure in absence (dashed lines) and presence of ions (solid lines).

Next we analyze the effect of using different CTLs, which in turn modify the value of the discontinuities ΔE_C and ΔE_V at the ETL/perovskite and perovskite/HTL interfaces, respectively. For the sake of simplicity, we only show the results corresponding to the ETL/perovskite interface. Similar conclusions are obtained for the perovskite/HTL interface. ETLs with different values of the electro-affinity are considered in the simulation. A different electro-affinity of the n-type conductor layer modifies ΔE_C, and hence the built-in potential $V_{bi\,ETL}$ of the ETL/perovskite heterojunction. The resulting energy diagrams are depicted in Figure 4, showing that the larger ΔE_C is, the more holes accumulate at the perovskite close to the interface with the ETL.

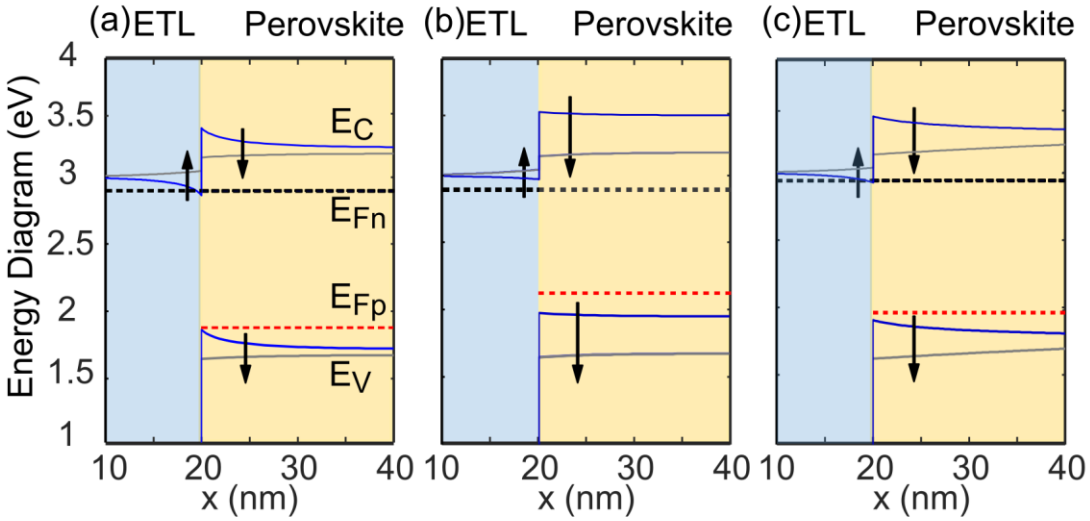

Figure 4. Energy diagrams of ETL/perovskite heterojunctions with different values of ΔE_C working at OC. The signs of the arrows indicate the effect of the decrement of

ΔE_C , from 0.5 to 0.1 eV. The following situations are shown: (a) No interfacial and low bulk recombination value (B_B = 10^{-14} cm^3/s); (b) high interfacial recombination (B_S = 10^{-12} cm^3/s) and low bulk recombination value (B_B = 10^{-14} cm^3/s) (c) no interfacial recombination and high bulk recombination (B_B = 10^{-4} cm^3/s, two orders higher than the Langevin recombination factor $q\mu/(\varepsilon_r\varepsilon_0) \approx 10^{-6}$ cm^3/s). Table S1 shows the rest of physical parameters used in the simulations. The values of the hole and electron densities at the ETL/perovskite interface for these three figures are depicted in Figure S3.

The three cases represented in Figure 4 include an additional study with the bulk and interfacial recombination. As a competition between bulk and surface recombination exists, but it is difficult to discern experimentally, what we propose with this simulation is to quantify their relative effects. In a practical situation, the rate constants of the interfacial recombination (B_S) and bulk recombination (B_B) are different and thus, the flux for both types of recombination is correspondingly different; otherwise, one would not evidence an output voltage for these devices. For that reason, we considered three cases: one case when almost no type of recombination exists and two cases in which one type of recombination dominates. As expected, an increment of the bulk recombination or the interfacial recombination flattens the bands and reduces the accumulation of charge at the interface. This reduction of the accumulation of charge is stronger for the interfacial recombination mechanism. The evolution with ΔE_C of the hole and electron densities at the ETL/perovskite interface for the three cases of Figure 4 is depicted in Figure 5.

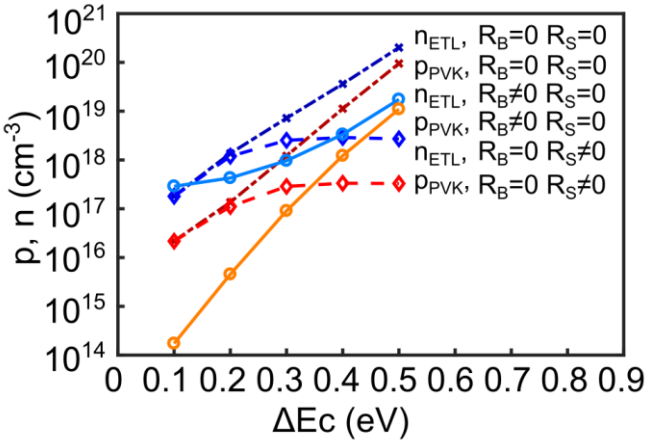

Figure 5. Evolution with ΔE_C of the hole and electron densities at the ETL/perovskite interface for the three cases of Figure 4 (main text): (a) Neither interfacial nor bulk recombination ($R_S = 0, R_B = 0$); (b) high interfacial recombination and low bulk recombination ($R_S \neq 0, R_B = 0$); and (c) no interfacial recombination and high bulk recombination ($R_S = 0, R_B \neq 0$).

As different perovskite materials and processes are used in the fabrication of PSCs, the values of the carrier mobility can differ up to two orders of magnitude.[32] In this regard, we have considered values of 1 and 100 cm^2/Vs for the carrier mobility in the perovskite. The increment of the value of the mobility favors the transport and extraction of free charge, which produces a flattening of the energy band and a decrement of the accumulation of charge of almost one order of magnitude (see Figure S5 in SI).

The different ETLs employed in typical PSCs also have different values of the relative permittivity.[33] From our numerical simulations, it is observed that an increment of the relative permittivity of the ETL makes the accumulation of free charge at the ETL/perovskite interface increase (electrons in the ETL side and holes in the perovskite side of the interface).

In summary, a strong accumulation of electrons and holes at each side of the ETL/perovskite interface is formed naturally in the OC steady state without previous treatments or preconditions, within the ranges of the following physical parameters: (1) a medium or high discontinuity of the ETL and perovskite conduction bands ($\Delta E_C \geq 0.2$ eV), (2) medium or low intensities of the interfacial and bulk recombination mechanisms, and (3) medium or low values of the free carrier mobility in the perovskite.

3.2. Short-circuit Condition

In this section, we simulate the performance of the ETL/perovskite/HTL structure at SC. The values of the parameters used in this simulation coincide with the ones used in OC (Table S1 in SI). The energy diagrams of the ETL/perovskite/HTL structure and the distributions of electrons, holes and ions along the structure, for high and low values of the on-average concentration of mobile ions N_{ion}, are depicted in Figure 6 and 7, respectively. The comparison of Figures 6b and 7b shows how the decrement of the ion concentration makes the accumulation of electrons and holes increase at the perovskite/HTL interface. The high accumulation of charge observed experimentally in capacitance measurements at SC can be attributed to the built-in potential of the perovskite/CTL heterojunctions. Electrons accumulate at the perovskite side of the HTL/perovskite interface because of the existing high energy barrier at this interface. Physically, the electron current is hindered and cannot flow through the interface towards the HTL side by the contact selectivity. On the contrary, holes are extracted towards the HTL side of the interface and accumulate due to the existing discontinuities before contacting of the energy valence bands and Fermi levels of each material of the HTL/perovskite interface. The reciprocal type of hole accumulation occurs at ETL/perovskite interface. These findings explain the high capacitances measured even at short circuit conditions.[9]

The main effect of increasing the concentration of ions is observed at the perovskite/HTL interface, its origin is found at the ETL/perovskite interface (see Figures

6a and 7a). In the case of a high concentration of ions, the anions accumulate close to the ETL/perovskite interface. This ionic charge screens the built-in field of this heterojunction, making the bands flatten in the perovskite and also making the remaining built-in potential drop mainly along the ETL. In the case of a low concentration of ions, the anions do not alter the existing built-in field in the ETL/perovskite heterojunction. The potential drops mainly along the perovskite semiconductor (the lowest doped material of both ETL and perovskite). In the study of Figures 6-7, low values of interfacial and bulk recombination are used in the simulation. Higher values of the interfacial and bulk recombination flatten the bands and reduce the accumulation of free charge, just like what is observed at the ETL/perovskite interface in OC when the recombination parameters are increased.

A study in SC of how the carrier mobility in the perovskite affects the accumulation of charge at the perovskite/HTL interface, leads to the same conclusions of the previous section. In the case of the carrier mobility in the HTL, it is worth mentioning that the HTL is typically an organic material, with a lower value of the carrier mobility than that of the perovskite semiconductor. In this regard, if the organic layer is too long, the extraction of charge can be hindered and the HTL would act as a bottleneck to the flow of charge. In addition, when the carrier mobility in the HTL decreases, transport resistance increases, and a higher voltage drop takes place in the HTL.

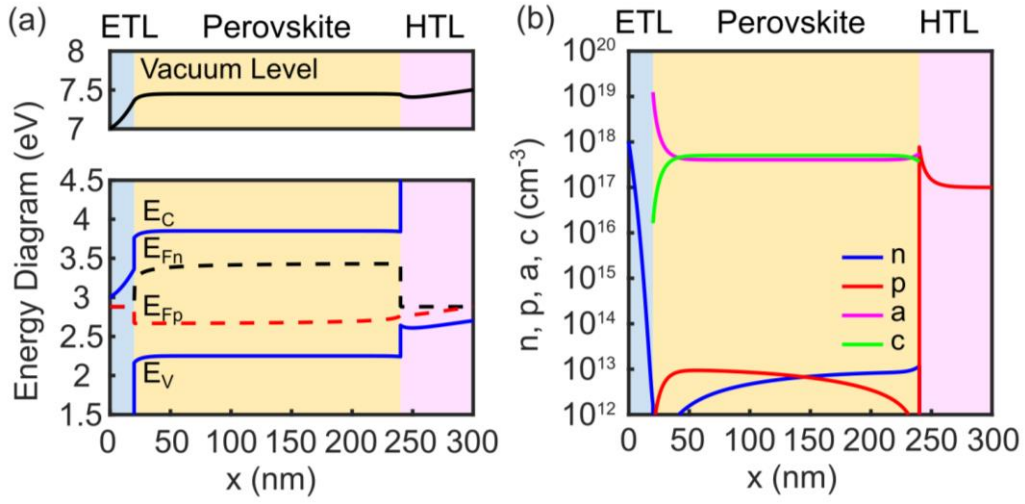

Figure 6. (a) Energy diagram of an ETL/perovskite/HTL structure at SC in steady-state ($V_{app} = 0\,\mathrm{V}$). (b) Distributions of electrons, holes and ions along the structure. A high on-average concentration of ions of $N_{ion} = 5\times10^{17}\,\mathrm{cm}^{-3}$ is considered in the perovskite.

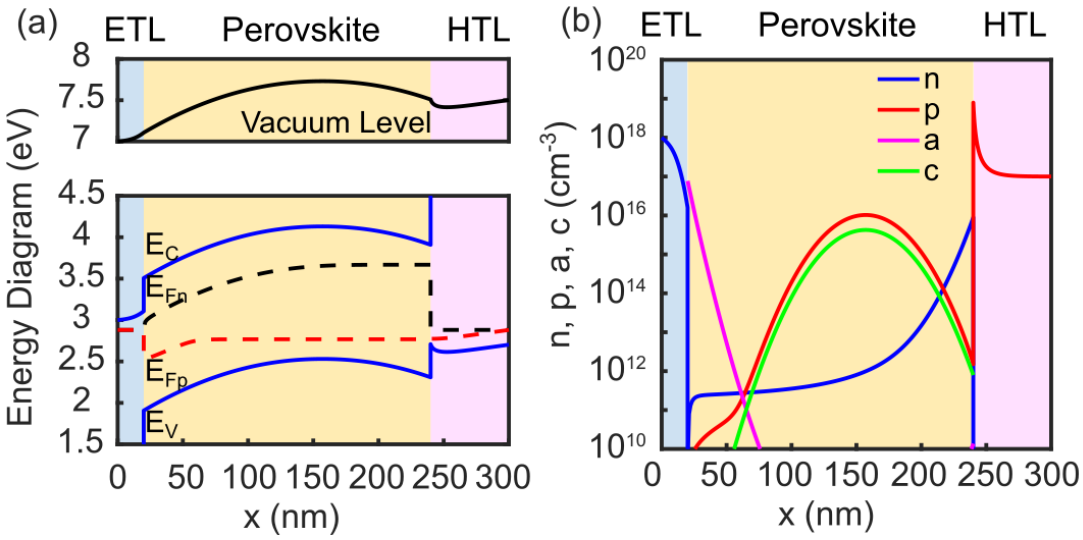

Figure 7. (a) Energy diagram of an ETL/perovskite/HTL structure at SC in steady-state ($V_{app} = 0\,\mathrm{V}$). (b) Distributions of electrons, holes and ions along the structure. A low on-average concentration of ions of $N_{ion} = 10^{15}\ \mathrm{cm}^{-3}$ is considered in the perovskite.

Conclusion

In this work, we have simulated numerically the ETL/perovskite/HTL structure of a perovskite solar cell at open-circuit and short-circuit. We have detected the existence of free charge accumulation at the interfaces of this structure and have quantified this accumulation of charge as a function of the device and material parameters, and as a function of mobile ion density. At OC, the accumulation of charge is located at both CTL/perovskite interfaces, while at SC, the free charge accumulates mainly at the perovskite/HTL interface for p-type perovskites and at the ETL/perovskite interface for n-type perovskites. The accumulation of electrons and holes at each side of the interfaces is formed naturally without previous treatments or preconditions. These accumulations of charge are consistent with the high values of the low-frequency capacitance observed in capacitance experiments. The presence of mobile ions only modifies the value of the accumulated charge.

Supporting Information

Energy diagrams of the charge-transport-layer/perovskite heterojunctions; numerical model of the surface recombination at the perovskite solar cell; influence of the discontinuity at the conduction band and the surface recombination on the free charge densities at the ETL/perovskite interface; short-circuit and open-circuit simulations of an n-type perovskite solar cell; influence of free charge carrier mobility on the accumulation of free charge carriers.

Acknowledgments
We acknowledge funding from MINECO of Spain under Project MAT2016-76892-C3-1-R, MAT2016-76892-C3-3-R and Universidad de Granada under the Grant *Contrato Puente*.

References

(1) Kojima, A.; Teshima, K.; Shirai, Y.; Miyasaka, T. Organometal halide perovskites as visible-light sensitizers for photovoltaic cells, *J. Am. Chem. Soc.* **2009**, 131, 6050-6051.

(2) Lopez-Varo, P.; Jiménez-Tejada, J. A.; García-Rosell, M.; Ravishankar, S.; Garcia-Belmonte, G.; Bisquert, J.; Almora, O. Device physics of hybrid perovskite solar cells: theory and experiment. *Adv. En. Mater.* **2018**, 1702772.

(3) Lopez-Varo, P.; Bertoluzzi, L.; Bisquert, J.; Alexe, M.; Coll, M.; Huang, J.; Jimenez-Tejada, J. A.; Kirchartz, T.; Nechache, R.; Rosei, F. et al. Physical aspects of ferroelectric semiconductors for photovoltaic solar energy conversion. *Phys. Rep.* **2016**, *653*, 1-40.

(4) Correa-Baena, J.-P.; Saliba, M.; Buonassisi, T.; Grätzel, M.; Abate, A.; Tress, W.; Hagfeldt, A. Promises and challenges of perovskite solar cells. *Science* **2017**, *358*, 739-744.

(5) van Reenen, S.; Kemerink, M.; Snaith, H. J. Modeling anomalous hysteresis in perovskite solar cells. *J. Phys. Chem. Lett.* **2015**, *6*, 3808-3814.

(6) Zarazua, I.; Bisquert, J.; Garcia-Belmonte, G. Light-induced space-charge accumulation zone as photovoltaic mechanism in perovskite solar cells. *J. Phys. Chem. Lett.* **2016**, *7*, 525-528.

(7) Kim, H.-S.; Jang, I.-H.; Ahn, N.; Choi, M.; Guerrero, A.; Bisquert, J.; Park, N.-G. Control of I–V hysteresis in $CH_3NH_3PbI_3$ perovskite solar cell. *J. Phys. Chem. Lett.* **2015**, *6*, 4633-4639.

(8) Lopez-Varo, P.; Jiménez-Tejada, J. A.; García-Rosell, M.; Anta, J. A.; Ravishankar, S.; Bou, A.; Bisquert, J. Effects of ion distributions on charge collection in perovskite solar cells. *ACS Energy Lett.* **2017**, 1450-1453.

(9) Zarazua, I.; Han, G.; Boix, P.P.; Mhaisalkar, S.G.; Fabregat-Santiago, F.; Mora-Seró, I.; Bisquert, J.; Garcia-Belmonte, G. Surface Recombination and Collection Efficiency in Perovskite Solar Cells from Impedance Analysis. *J. Phys. Chem. Lett.* **2016**, *7*, 5105-5113.

Surface Recombination and Collection Efficiency in Perovskite Solar Cells from Impedance Analysis.

(10) Jiang, C.-S.; Yang, M.; Zhou, Y.; To, B.; Nanayakkara, S. U.; Luther, J. M.; Zhou, W.; Berry, J. J.; van de Lagemaat, J.; Padture, N. P. et al. Carrier separation and transport in perovskite solar cells studied by nanometre-scale profiling of electrical potential. *Nat. Commun.* **2015**, *6*, 8397.

(11) Bergmann, V. W.; Guo, Y.; Tanaka, H.; Hermes, I. M.; Li, D.; Klasen, A.; Bretschneider, S. A.; Nakamura, E.; Berger, R.; Weber, S. A. L. Local time-

dependent charging in a perovskite solar cell. *ACS Appl. Mater. Int.* **2016**, *8*, 19402-19409.

(12) Cai, M.; Ishida, N.; Li, X.; Yang, X.; Noda, T.; Wu, Y.; Xie, F.; Naito, H.; Fujita, D.; Han, L. Control of electrical potential distribution for high-performance perovskite solar cells. *Joule* **2018**, *2*, 296-306.

(13) Belisle, R. A.; Nguyen, W. H.; Bowring, A. R.; Calado, P.; Li, X.; Irvine, S. J. C.; McGehee, M. D.; Barnes, P. R. F.; O'Regan, B. C. Interpretation of inverted photocurrent transients in organic lead halide perovskite solar cells: proof of the field screening by mobile ions and determination of the space charge layer widths. *Energy Environ. Sci.* **2017**, *10*, 192-204.

(14) Eames, C.; Frost, J. M.; Barnes, P. R. F.; O'Regan, B. C.; Walsh, A.; Islam, M. S. Ionic transport in hybrid lead iodide perovskite solar cells. *Nat. Commun.* **2015**, *6*.

(15) Calado, P.; Telford, A. M.; Bryant, D.; Li, X.; Nelson, J.; O'Regan, B. C.; Barnes, P. R. F. Evidence for ion migration in hybrid perovskite solar cells with minimal hysteresis. *Nat. Commun.* **2016**, *7*, 13831.

(16) Foster, J. M.; Snaith, H. J.; Leijtens, T.; Richardson, G. A model for the operation of perovskite based hybrid solar cells: formulation, analysis, and comparison to experiment. *SIAM J. Appl. Math.* **2014**, *74*, 1935-1966.

(17) Xue, H.; Fu, K.; Wong, L. H.; Birgersson, E.; Stangl, R. Modelling and loss analysis of meso-structured perovskite solar cells. *J. Appl. Phys.* **2017**, *122*, 083105.

(18) Richardson, G.; O'Kane, S. E. J.; Niemann, R. G.; Peltola, T. A.; Foster, J. M.; Cameron, P. J.; Walker, A. B. Can slow-moving ions explain hysteresis in the current-voltage curves of perovskite solar cells? *Energy Environ. Sci.* **2016**, *9*, 1476-1485.

(19) Huang, Y.; Aharon, S.; Rolland, A.; Pedesseau, L.; Durand, O.; Etgar, L.; Even, J. Influence of schottky contact on the C-V and J-V characteristics of HTM-free perovskite solar cells. *EPJ Photovolt.* **2017**, *8*, 85501.

(20) Domanski, K.; Roose, B.; Matsui, T.; Saliba, M.; Turren-Cruz, S.-H.; Correa-Baena, J.-P.; Carmona, C. R.; Richardson, G.; Foster, J. M.; De Angelis, F. et al. Migration of cations induces reversible performance losses over day/night cycling in perovskite solar cells. *Energy Environ. Sci.* **2017**, *10*, 604-613.

(21) Senocrate, A.; Moudrakovski, I.; Kim, G. Y.; Yang, T.-Y.; Gregori, G.; Grätzel, M.; Maier, J. The nature of ion conduction in methylammonium lead iodide: a multimethod approach. *Angew. Chem. Int. Ed.* **2017**, *56*, 7755-7759.

(22) Li, C.; Guerrero, A.; Zhong, Y.; Gräser, A.; Luna, C. A. M.; Köhler, J.; Bisquert, J.; Hildner, R.; Huettner, S. Real-time observation of iodide ion migration in

methylammonium lead halide perovskites. *Small* **2017**, *13*, 1701711.

(23) Almora, O.; Guerrero, A.; Garcia-Belmonte, G. Ionic charging by local imbalance at interfaces in hybrid lead halide perovskites. *Appl. Phys. Lett.***2016**, *108*, 043903.

(24) Tress, W.; Yavari, M.; Domanski, K.; Yadav, P.; Niesen, B.; Correa Baena, J. P.; Hagfeldt, A.; Graetzel, M. Interpretation and evolution of open-circuit voltage, recombination, ideality factor and subgap defect states during reversible light-soaking and irreversible degradation of perovskite solar cells. *Energy Environ. Sci.* **2018**, *11*, 151-165.

(25) Wojciechowski, K.; Stranks, S. D.; Abate, A.; Sadoughi, G.; Sadhanala, A.; Kopidakis, N.; Rumbles, G.; Li, C.-Z.; Friend, R. H.; Jen, A. K. Y. et al. Heterojunction modification for highly efficient organic-inorganic perovskite solar cells. *ACS Nano* **2014**, *8*, 12701-12709.

(26) Gottesman, R.; Lopez-Varo, P.; Gouda, L.; Jimenez-Tejada, Juan A.; Hu, J.; Tirosh, S.; Zaban, A.; Bisquert, J. Dynamic phenomena at perovskite/electron-selective contact interface as interpreted from photovoltage decays. *Chem* **2016**, *1*, 776-789.

(27) Calió, L.; Kazim, S.; Grätzel, M.; Ahmad, S. Hole-transport materials for perovskite solar cells. *Angew. Chem. Int. Ed.* **2016**, *55*, 14522-14545.

(28) Mahmood, K.; Sarwar, S.; Mehran, M. T. Current status of electron transport layers in perovskite solar cells: materials and properties. *RSC Advances* **2017**, *7*, 17044-17062.

(29) Gagliardi, A.; Abate, A. Mesoporous electron-selective contacts enhance the tolerance to interfacial ion accumulation in perovskite solar cells. *ACS Energy Letters* **2018**, *3*, 163-169.

(30) López-Varo, P.; Jiménez-Tejada, J. A.; Marinov, O.; Carceller, J. E.; Chen, C. H.; Deen, M. J. Boundary condition model for the simulation of organic solar cells. *Organic Electronics* **2017**, *48*, 85-95.

(31) Bisquert, J. *The physics of solar cells: perovskites, organics, and photovoltaic fundamentals*; CRC Press, **2017**.

(32) Herz, L. M. Charge-carrier mobilities in metal halide perovskites: fundamental mechanisms and limits. *ACS Energy Lett.* **2017**, *2*, 1539-1548.

(33) Schneemeyer, L. F.; van Dover, R. B.; Fleming, R. M. High dielectric constant Hf–Sn–Ti–O thin films. *Appl. Phys. Lett.* **1999**, *75*, 1967-1969.

TOC Graphic.

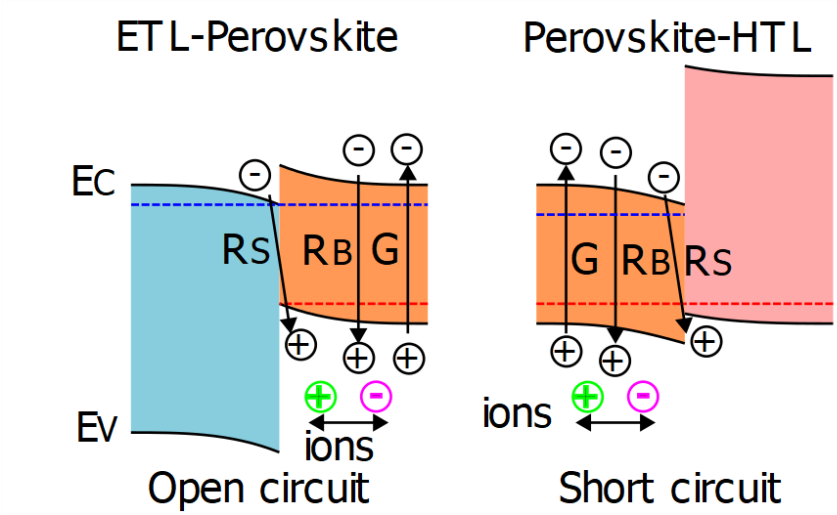
ETL-Perovskite
Perovskite-HTL
Ec
Ev
RS
RB
G
ions
Open circuit
G
RB
RS
ions
Short circuit